

**Seismic and structural assessment of the perry memorial arch using finite element modeling****Harshitha Peddakanti<sup>a</sup>, Ashok Gyawali<sup>b</sup> and Byungik Chang<sup>c\*</sup>**<sup>a</sup>Structural Engineer, Hudson Engineering, LLC, Bayonne, NJ 07002, USA<sup>b</sup>Civil Engineer, WSP, Valhalla, NY 10595, USA<sup>c</sup>Professor, Department of Civil and Environmental Engineering, University of New Haven, West Haven, CT, 06516, USA**ARTICLE INFO***Article history:*

Received 10 January 2026

Accepted 22 February 2026

Available online

22 February 2026

*Keywords:**Perry Memorial Arch**Historic masonry structures**Seismic analysis**Dynamic loading**Finite element modeling***ABSTRACT**

Historic masonry monuments are particularly vulnerable to dynamic loading due to aging materials, limited ductility, and the absence of seismic design considerations. This study presents a numerical assessment of the Perry Memorial Arch, a historic masonry structure located in Bridgeport, Connecticut, under gravity, wind, and seismic loading conditions. A three-dimensional finite element model was developed in ANSYS to evaluate stress distribution, deformation patterns, and dynamic response using static analysis, modal analysis, and nonlinear time-history analysis. The structure was modeled using macro-level material representations for stone masonry, brick masonry, and concrete, with material properties derived from code-based references due to the absence of in-situ testing data. Wind loading was evaluated in accordance with ASCE 7-16, while seismic performance was assessed using location-specific spectral parameters and selected ground-motion records with Peak Ground Accelerations (PGA) ranging from 0.10g to 0.16g. Results indicate that the arch performs satisfactorily under gravity and wind loading, although stress concentrations develop near supports under extreme wind conditions. Seismic analysis shows that the structure remains stable for PGA values up to 0.12g, while higher intensities lead to localized stress amplification, particularly in the in-plane direction. This study provides a screening-level seismic performance assessment of a historic masonry monument in a moderate seismic region and offers insights to support future retrofit planning and preservation strategies for similar heritage structures.

© 2026 Growing Science Ltd. All rights reserved.

**1. Introduction**

Monumental buildings constitute an essential part of cultural heritage worldwide, representing historical, architectural, and societal values that warrant long-term preservation. Significant efforts have therefore been devoted to understanding the structural behavior of such monuments, particularly because many were constructed using limited material knowledge and in the absence of modern design codes, which has contributed to progressive deterioration over time (De Angelis, 2020). The classification of a structure as historic varies by country and cultural context, and not all aged buildings are automatically considered heritage assets. In the United States, the National Park Service defines a historic structure as one that is more than 50 years old and either listed in, or eligible for, the National Register of Historic Places, or designated at the state or local level as an individual structure or a contributing element within a historic district. This designation has enabled the preservation and restoration of numerous monuments through coordinated efforts between federal, state, and local organizations.

Conservation may be broadly defined as a set of practices aimed at safeguarding heritage assets for future generations, restoring existing damage, and preventing the development of new structural deficiencies. Historic masonry structures, in particular, present unique challenges. Unreinforced masonry systems are typically well suited to resist gravity loads but are inherently vulnerable to horizontal actions, including wind and seismic forces. Even low-intensity earthquakes can lead to cracking, loss of integrity, and partial or global collapse in such structures (Puncello & Caprili, 2023). As a result, conservation

\* Corresponding author.

E-mail addresses: [bchang@newhaven.edu](mailto:bchang@newhaven.edu) (B. Chang)

ISSN 2291-8752 (Online) - ISSN 2291-8744 (Print)

© 2026 Growing Science Ltd. All rights reserved.

doi: 10.5267/j.esm.2026.2.001

strategies often include repair and strengthening techniques such as repointing of masonry joints, introduction of bearing plates, cement grouting of cracks, localized sheathing, and, where appropriate, the addition of shear-resisting elements.

The Perry Memorial Arch (**Fig. 1**), located in Bridgeport, Connecticut, was selected as the case study for this research. The monument has experienced noticeable deterioration due to prolonged exposure to environmental conditions, resulting in cracking of stone and brick masonry, degradation of mortar joints, and partial separation of transverse walls. Prior to rehabilitation, a thorough structural assessment is required to evaluate the integrity and safety of the arch. Given its masonry construction, stress analysis under multiple loading scenarios is necessary to characterize its response and identify critical vulnerabilities. In historic masonry, axial compressive stresses induced by gravity loads may be of the same order of magnitude as the compressive capacity of aged materials. When combined with dynamic actions such as earthquakes, these stresses can trigger severe damage and localized failure mechanisms.



**Fig. 1.** Perry Memorial Arch located in Bridgeport, Connecticut

The seismic vulnerability assessment of historic masonry structures is widely recognized as a complex task due to uncertainties associated with material properties, geometry, boundary conditions, and construction techniques (De Angelis, 2020). Each historic masonry building has a unique construction history shaped by successive modifications, repairs, and material replacements. Consequently, reliable structural analysis requires a comprehensive understanding of the structure's geometry, historical evolution, construction details, cracking patterns, and damage distribution (Betti et al., 2012). To support dynamic characterization, complementary techniques such as ambient vibration testing and modal analysis have been extensively applied to heritage structures, providing valuable information on natural frequencies and mode shapes that can inform numerical modeling and retrofit strategies (Brandão, 2018).

Numerical methods, particularly finite element modeling, have become a common tool for evaluating the seismic behavior of historic masonry. For example, Betti and Galano (2012) investigated the seismic vulnerability of the Vicarious Palace in Pescia, Italy, using a nonlinear finite element model and pushover analysis in accordance with Italian technical guidelines. Their results demonstrated the fragility of the structure and its susceptibility to extensive damage under seismic loading, highlighting the importance of such analyses for retrofit planning. Similarly, Özmen and Sayin (2018) analyzed the seismic response of a historic masonry arch bridge in Maden, Turkey, using three-dimensional finite element modeling in ANSYS and time-history analysis based on recorded earthquake motions. Their study provided detailed insight into stress, strain, and displacement demands during seismic events.

Despite its historical significance and visible deterioration, no comprehensive structural assessment of the Perry Memorial Arch has been conducted to evaluate its response to combined gravity, wind, and seismic loading. In particular, the seismic vulnerability of historic masonry monuments located in moderate-seismicity regions of the northeastern United States remains insufficiently documented. This study addresses this gap by providing a screening-level numerical assessment of the Perry Memorial Arch using finite element modeling.

Numerical methods, particularly finite element modeling, have become widely used for evaluating the seismic performance of historic masonry structures. For instance, Betti and Galano (2012) examined the seismic vulnerability of the Vicarious Palace in Pescia, Italy, using nonlinear finite element modeling combined with pushover analysis in accordance with Italian technical guidelines. Their findings highlighted the structural fragility and susceptibility to severe damage under seismic loading, emphasizing the importance of numerical analyses in retrofit planning. Similarly, Özmen and Sayin (2018) investigated the seismic response of a historic masonry arch bridge in Maden, Turkey, through three-dimensional finite element modeling in ANSYS and time-history analysis based on recorded earthquake motions, providing detailed insight into stress, strain, and displacement demands during seismic events. In addition, finite element modeling has been extensively applied to other structural systems, including bridges (Chang et al., 2015; Chanmalai et al., 2021), overhead support structures

(Chang et al., 2014; Ong et al., 2020), and seismic dampers (Thongchom et al., 2022), demonstrating its broad applicability in structural performance assessment.

The motivation for this research arises from the increasing exposure of historic monuments to natural and anthropogenic hazards, including seismic activity and climate-driven environmental degradation. As extreme weather events become more frequent and infrastructure systems age, the need to understand the structural performance of heritage assets under combined loading scenarios has become more urgent.

The objectives of this study are to: (1) evaluate the structural response of the Perry Memorial Arch under gravity and wind loading; (2) assess the dynamic characteristics and seismic response of the arch using nonlinear finite element analysis; (3) identify critical stress concentrations and deformation patterns under varying Peak Ground Acceleration values; and (4) provide a screening-level assessment to inform future monitoring and retrofit strategies.

The novelty of this study lies in the combined assessment of gravity, wind, and seismic loading for a historic masonry monument located in a moderate-seismicity region of the northeastern United States. Unlike many previous investigations focused on high-seismic zones, this work provides a screening-level evaluation of structural performance using ground motions representative of the U.S. East Coast. The results are intended to support preservation-oriented decision-making and inform future retrofitting and reinforcement strategies for similar heritage masonry structures.

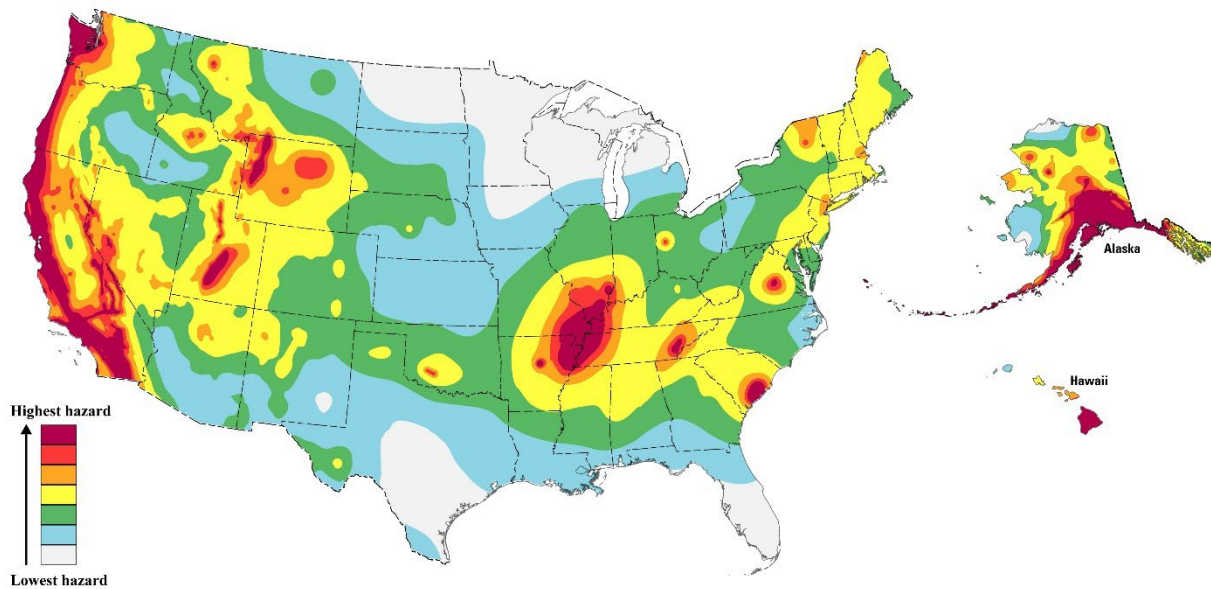


Fig. 2. Simplified USGS seismic hazard map for the United States (USGS, 2023)

## 2. Methodology

This section describes the geometric characteristics of the Perry Memorial Arch and the numerical methodology adopted to evaluate its structural response under static, wind, and seismic loading conditions. The overall approach is based on three-dimensional finite element modeling, allowing for assessment of stress distribution, deformation patterns, and dynamic response under various loading scenarios. A three-dimensional finite element framework was used to ensure consistent comparison of responses across all load cases.

### 2.1 Description of the Structure

The Perry Memorial Arch is located in Seaside Park, Bridgeport, Connecticut, and was constructed in 1918 as a commemorative monument. It is recognized as one of Connecticut's historic landmarks. Over time, the structure has exhibited significant deterioration, including cracking in stone and brick masonry, degradation of mortar joints due to prolonged moisture exposure during winter and seasonal storms, and vegetation growth on exterior surfaces. In response to these conditions, Fairfield County has initiated plans to retrofit the structure as a proactive preservation measure. These observed conditions motivate a numerical investigation to establish baseline structural behavior prior to rehabilitation.

The arch is a masonry structure consisting primarily of granite stone masonry on the exterior walls and brick masonry of varying thickness on the interior. The exterior configuration comprises a spandrel arch, while the interior includes a vaulted arch system with interior brick walls and openings. The roof system consists of reinforced concrete slabs with cinder concrete filling and granite slab topping. A representative sectional view illustrating the material composition is shown in **Fig. 3**.

The principal geometric dimensions of the structure are summarized in **Table 1**. These dimensions were used to develop the numerical model and to define material volumes and load application areas.

**Table 1.** Geometrical description of the Perry Memorial Arch.

No	Description	Dimensions (ft)
1	Height of the Structure	56'-8"
2	Width	14'-6"
3	Length	84'-6"
4	Thickness of the Granite wall	1'
5	Thickness of Brick wall	1'-6"
6	Thickness of Reinforced Concrete Slab	1'-6"

Note: 1' = 0.3048m, 1" = 0.0254m

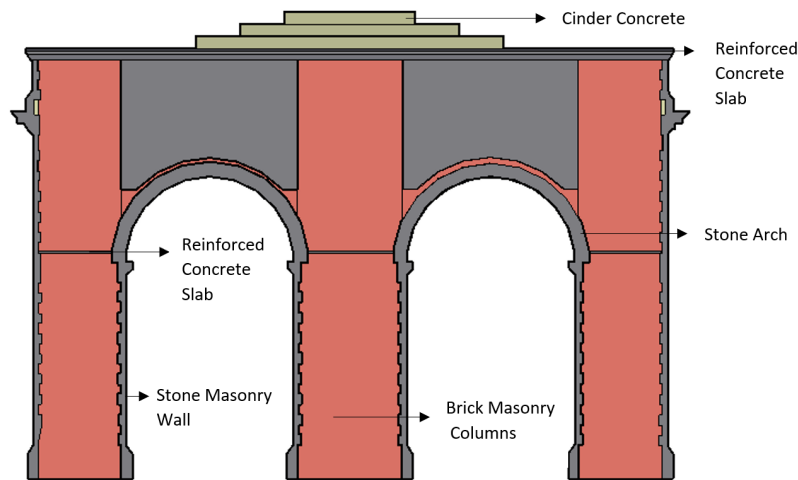


**Fig. 3.** Section view showing material composition.

## 2.2 Finite Element Modelling Approach

A three-dimensional nonlinear finite element (FE) model of the Perry Memorial Arch was developed using ANSYS to evaluate its structural behavior under static and dynamic loading conditions. The modeling process began with the creation of a detailed three-dimensional CAD representation of the structure, which was subsequently imported into the ANSYS environment. The analysis framework included:

- Static structural analysis under gravity loading,
- Static analysis including wind pressure,
- Modal analysis to determine natural frequencies and mode shapes, and
- Nonlinear transient dynamic analysis to simulate earthquake-induced ground motions.

This sequencing allows the gravity-induced stress state to be carried into wind and seismic analyses, which is important for nonlinear response evaluation.

Static analysis results were compared with theoretical load estimates derived in accordance with ASCE 7-16 to verify model consistency. Modal analysis was conducted to support dynamic characterization of the structure and to provide insight into dominant vibration modes, which is particularly important for historic masonry systems. Transient structural analysis was then used to evaluate seismic response under multiple earthquake scenarios with varying Peak Ground Acceleration (PGA) levels.

Depending on the desired level of detail, masonry structures can be modeled using detailed micro-modeling, simplified micro-modeling, or macro-modeling approaches (Asikoglu, 2019). In this study, a macro-modeling approach was adopted, in which masonry components are represented as homogeneous continua with equivalent material properties. This approach provides an effective balance between computational efficiency and the ability to capture global structural behavior, making it suitable for screening-level assessment of large historic monuments.

### 2.3 Element Types and Contact Modeling

Several element types available in the ANSYS element library were used to represent the structural components of the arch. SOLID186 and SOLID187 elements were employed to model the volumetric behavior of stone masonry, brick masonry, and concrete components. These higher-order solid elements are well suited for capturing stress gradients and deformation in irregular geometries. Contact interactions between adjoining structural components were modeled using CONTA174 elements to represent interface compatibility and potential separation/sliding behavior where applicable.

### 2.4 Meshing Strategy

Meshing plays a critical role in achieving accurate finite element simulations. In finite element analysis, the mesh discretizes the structure into smaller elements connected at nodes, each defined by spatial coordinates. This discretization allows complex geometries to be analyzed numerically by approximating their behavior using a system of equations (Cook, 2001). A mesh sensitivity study was performed to confirm that additional refinement did not materially change global stress or deformation trends.

Given the complex geometry of the Perry Memorial Arch, an adaptive meshing strategy with a relatively uniform element size was adopted. Automatic meshing techniques, including tetrahedral and hex-dominant elements, were employed to ensure adequate representation of curved surfaces and internal features. The mesh was refined sufficiently to capture stress concentrations while maintaining reasonable computational efficiency. The resulting meshed model is shown in Fig. 4 and Fig. 5.

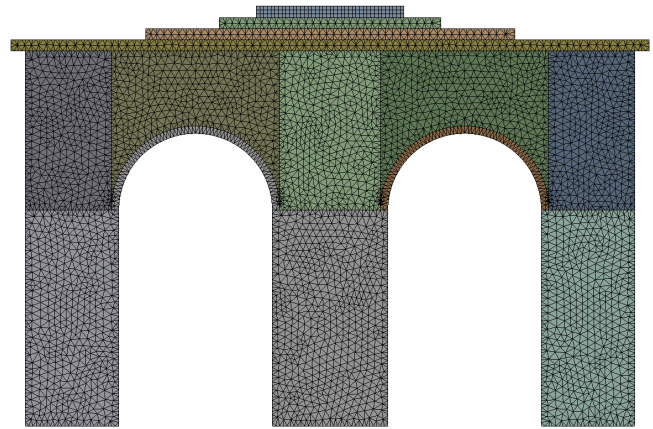
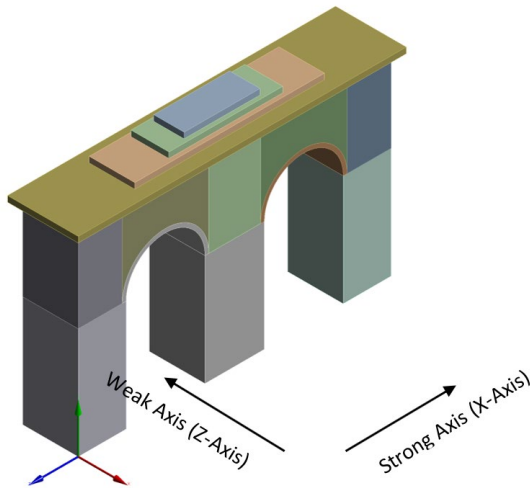


**Fig. 4.** Finite element model of the Perry Memorial Arch. **Fig. 5.** Finite element mesh of the Perry Memorial Arch

During the meshing process, SOLID186, SOLID187, and CONTA174 elements were generated automatically. SOLID186 and SOLID187 elements represent the continuum behavior of the structural materials, while CONTA174 elements define contact conditions between adjacent components (Zienkiewicz, 2013; Belytschko, 2014).

### 2.5 Material model and Boundary Conditions

As is common with historic masonry structures, detailed information regarding original material properties was not available. Consequently, material properties were assumed based on established code references and published literature. The structural components were categorized into stone masonry, brick masonry, and concrete, with corresponding mechanical properties summarized in Table 2.

**Table 2.** Material properties (AISC, 2017) (American Standard Building Code Requirements for Masonry, 1954)(ACI 213R)

Material	Stone Masonry	Brick Masonry	Concrete
Elastic Modulus (ksi)	$3.75 \times 10^2$	$2.1 \times 10^2$	$3.12 \times 10^3$
Density (lb/ft <sup>3</sup> )	137	112	115
Tensile Strength (ksi)	0.16	0.09	0.30
Compressive Strength (ksi)	0.5	0.3	3.0

Note: 1ksi = 6.895 MPa and 1lb/ft<sup>3</sup> = 157.08 N/m<sup>3</sup>

Density values for stone and brick masonry were obtained from AISC Table 17-12 (AISC, 2017). Structural low-density concrete properties were assumed in accordance with ACI 213R. Minimum compressive strength values for masonry were derived from the American Standard Building Code Requirements for Masonry. Since unreinforced masonry exhibits limited tensile capacity, tensile strength was estimated to be 33% of the compressive strength, consistent with established recommendations (Lourenco, 1996). Boundary conditions were defined by restraining all translational and rotational degrees of freedom at the piers, corresponding to fixed boundary conditions. This assumption reflects the substantial foundation

support provided by the massive masonry piers and is consistent with common practice in screening-level assessments of historic masonry monuments. While fixed supports may locally overestimate stiffness, this simplification is appropriate for a conservative screening-level evaluation of global response.

### 2.6 Seismic demand definition (ASCE 7-16)

The design spectral acceleration parameters for the Perry Memorial Arch were derived using resources from the California Office of Statewide Health and Planning Development (OSHPD), which provides USGS-based seismic design parameters applicable nationwide under ASCE 7-16. OSHPD collaborates with the Structural Engineers' Association of California (SEAOC) to utilize USGS web services for the creation of location-specific spectral maps. These values were computed in accordance with the directives specified in ASCE 7-16. The spectral acceleration parameters obtained for this study are displayed in **Table 3**. These parameters were used to define code-consistent seismic demand for response spectrum evaluation and to contextualize the selected time-history records. The seismic base shear is the total design lateral force at the base of a building. The Equivalent Lateral Force (ELF) procedure was used to calculate the seismic base shear based on ASCE 7-16. **Table 4** shows various parameters calculated to obtain the seismic base shear. The design response spectrum was plotted based on ASCE 7-16. **Table 5** presents the values used to generate the design response spectrum curve.

**Table 3:** Design spectral acceleration parameters for seismic analysis (ASCE, 2016)

Design Spectral Acceleration Parameters	Notes	
Seismic Design Category	B	
Mapped Spectra Acceleration ( $S_s$ )	0.211g	
Numeric Seismic Design Value ( $S_{DS}$ )	0.183g	0.2s SA
Numeric Seismic Design Value ( $S_{D1}$ )	0.073g	1.0s SA
Long-period Transition Period ( $T_L$ )	6 sec	
Response Modification Coefficient $\mathbb{R}$	1.5	
Importance Factor ( $I_c$ )	1	

**Table 4.** Parameters used for seismic base shear calculation (ASCE, 2016)

Seismic Parameters		
Short Period Ground motion ( $T_o$ )	0.08	sec
Characteristic Period of Ground Motion ( $T_s$ )	0.4	sec
Fundamental Period (T)	0.41	sec
Seismic Response Coefficient ( $C_s$ )	0.12	
Maximum Seismic Response Coefficient ( $C_{smax}$ )	0.12	
Minimum Seismic Response Coefficient ( $C_{smin}$ )	0.01	
Consider ( $C_s$ )	0.12	
Effective Seismic Weight (W)	3,063,500	lb
Seismic Base Shear (V)	360.3	kip

Note: 1lb = 0.453kg and 1kip = 4448.22 N.

**Table 5.** Design response spectrum values used in seismic analysis.

Period, T (sec)	Spectral Response Acceleration, $S_a$ (g)
0.00	0.073
0.08	0.183
0.40	0.183
1	0.048
6	0.008

## 3. Results and Discussions

### 3.1 Gravity Load Response (Pre-stress Condition)

A gravity-load analysis was first performed to establish a baseline stress state and to provide a pre-stress condition for subsequent wind and seismic analyses. The structure was assumed to be in serviceable condition, and fixed boundary conditions were applied at the base (piers) to restrain translations and rotations. A nonlinear static analysis accounting for large deflection effects was conducted. A standard gravitational acceleration of  $-386.09 \text{ in/s}^2$  was applied in the global Y-direction. This analysis establishes the initial stress field used in all subsequent load cases. **Fig. 6** summarizes the gravity-load response. Computed stresses were generally low across most regions of the arch, indicating that gravity loading alone does not govern structural demand. The maximum principal stress under self-weight was 51.84 psi, occurring at the interior side of the roof slab, while the maximum shear stress was 135.95 psi, concentrated at the corners of the brick and stone walls (**Table 6**). Directional deformation in the Y-direction was negligible (maximum approximately  $-0.08 \text{ in}$ ). Stress concentrations were most apparent at the spandrel region and at geometric discontinuities, consistent with expected behavior in masonry systems under gravity loading. These results confirm that the structure performs adequately under gravity loads and that additional load cases are required to activate critical response mechanisms.

**Table 6.** Summary of structural response under gravity loading

Load	Gravity	Location of Max Value
Maximum Principal Stress	51.836 psi	Interior side of roof slab
Maximum Shear Stress	135.95 psi	Corners of brick and stone walls
Directional Deformation-Y	-0.08 in	-

Note: 1 psi = 0.006894 N/mm<sup>2</sup>, 1 inch = 25.4mm

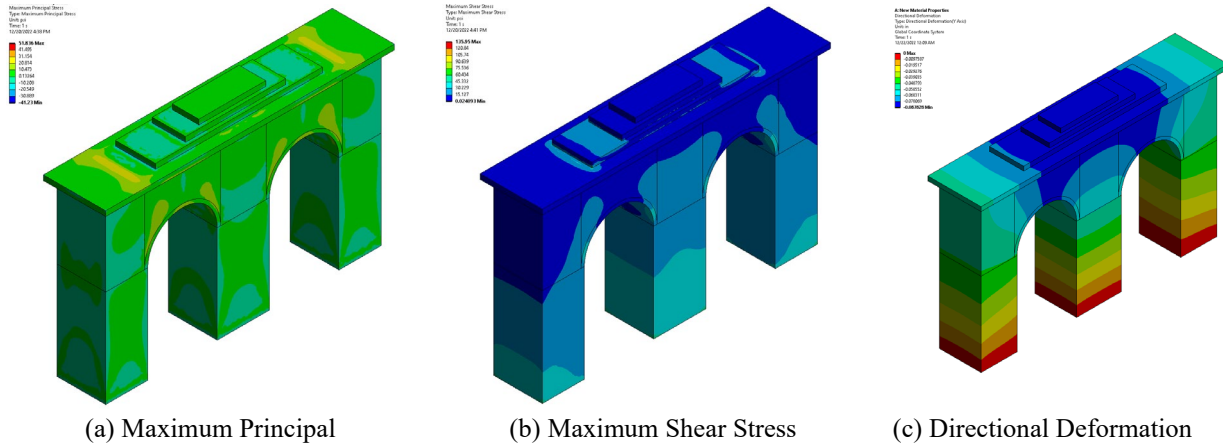


**Fig. 6.** Stress and deformation contours under gravity loading.

**3.2 Wind Load Response and Comparison with Code-Based Estimates**

Following the gravity-load assessment, wind loading was evaluated to examine lateral response and potential overturning behavior. The Perry Memorial Arch was evaluated under wind loading using both theoretical calculations (ASCE 7-16) and numerical finite element simulation. Based on ASCE 7-16, the basic wind speed at the site was taken as 108 mph, and the structure was classified as Risk Category I. The computed total structure weight based on unit weights and material volumes is presented in **Table 7**. The wind-exposed projected surface area was estimated from the CAD model as 2915.2 ft<sup>2</sup>.

**Table 7.** Calculated self-weight of the Perry Memorial Arch

Material	Unit Weight (lb/ft <sup>3</sup> )	Total Volume of Material (ft <sup>3</sup> )	Weight (kip)
Concrete	115.0	4008.0	460.9
Stone Masonry	137.0	8897.9	1218.9
Brick Masonry	112.0	12354.6	1383.7
Total Weight (kip)			3063.5

Note: 1lb/ft<sup>3</sup>= 157.08N /m<sup>3</sup>, 1ft<sup>3</sup>= 0.02831 m<sup>3</sup> and 1kip = 4448.22 N

The total wind force was calculated using ASCE 7-16. The velocity pressure, q<sub>z</sub>, evaluated at height z above ground, is defined as:

$$q_z = 0.00256K_zK_{zt}K_dK_eV^2 \text{ (lb/ft}^2\text{)}; V \text{ in mph} \tag{1}$$

Key wind parameters adopted from ASCE 7-16 are summarized in **Table 8**, and velocity pressure coefficients (K<sub>z</sub>) at representative heights are listed in **Table 9**. These parameters were used to incrementally apply wind pressures to the exterior surfaces of the FE model. Theoretical overturning checks indicated a maximum wind speed capacity of approximately 250 mph (111.76 m/s). Using the Main Wind Force Resisting System (MWFRS) approach, the maximum wind speed capacity was estimated at 266.1 mph. In the finite element simulation, the maximum principal stress at the theoretical overturning wind speed was approximately 201.3 psi, concentrated near the base. This value exceeds the assumed tensile strength of stone masonry (165 psi), suggesting that tensile cracking may initiate prior to global overturning. By progressively increasing applied wind pressure, the wind speed corresponding to tensile stress onset was estimated at approximately 239 mph. **Fig. 7** presents representative stress and deformation contours at this wind speed. Principal stress concentrations were greatest near the supports, while elevated shear stresses were also observed in the lower portions of the structure. These results indicate that wind-induced damage would likely initiate near the base and corners, rather than through global instability. The velocity pressure coefficient, K<sub>z</sub>, in **Table 9** is calculated at different heights of the structure, and the respective velocity pressure is evaluated for the same heights based on ASCE 7-16.

**Table 8.** Wind Load Parameters (ASCE, 2016)

Wind Load Parameters		Reference	
Wind directionality Factor (K <sub>d</sub> )	0.85	Section 26.6	Table 26.6-1
Exposure Category	D	Section 26.7	
Topographic Factor (K <sub>zt</sub> )	1.00	Section 26.8	Figure 26.8-1
Ground elevation factor (K <sub>e</sub> )	1.00	Section 26.9	

**Table 9.** Velocity Pressure Coefficient

Height, z (ft)	$K_z$
29.2	1.16
50.8	1.27
56.8	1.30

Note: 1ft = 0.3048 m

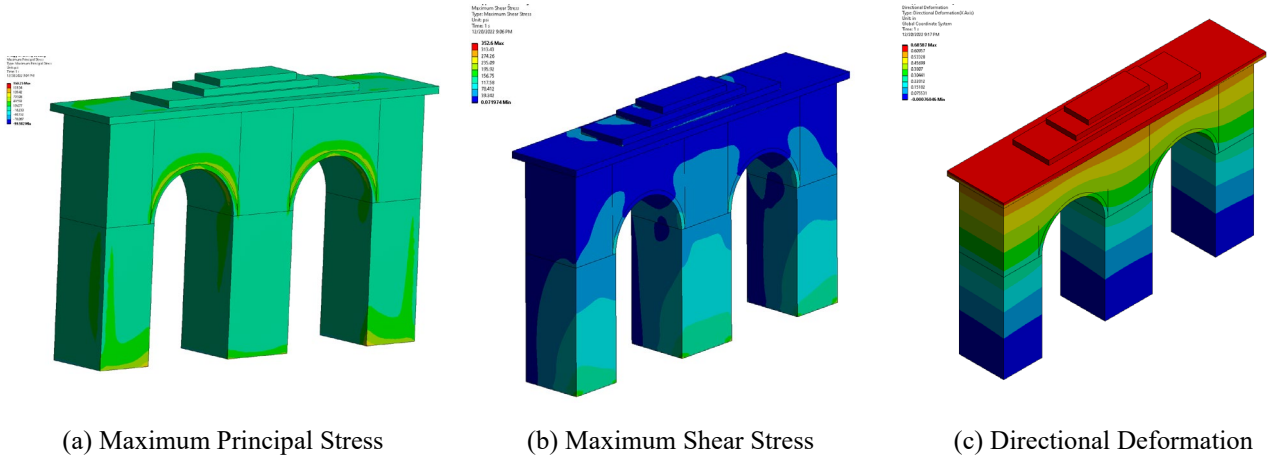


**Fig. 7.** Stress and deformation contours under lateral wind loading

3.3 Modal Characteristics (Pre-stressed Modal Analysis)

To characterize the dynamic properties of the structure prior to seismic excitation, a pre-stressed modal analysis was conducted (Fig. 8). The fundamental period estimated by hand calculation was 0.41 s, which compares well with the FE-based first-mode period of 0.43 s, indicating good agreement between simplified analytical estimates and the numerical model. Modal results indicate that a limited number of modes contribute significantly to overall dynamic response. The average effective mass participation ratio across the X, Y, and Z directions was approximately 0.86, and the first 20 modes collectively captured the majority of participating mass. The first mode exhibited dominant participation in the X direction (participation factor 71.67), the second mode in the Z direction (77.71), and the eighth mode in the Y direction (72.81). These findings guided interpretation of direction-dependent response observed in subsequent time-history analyses.

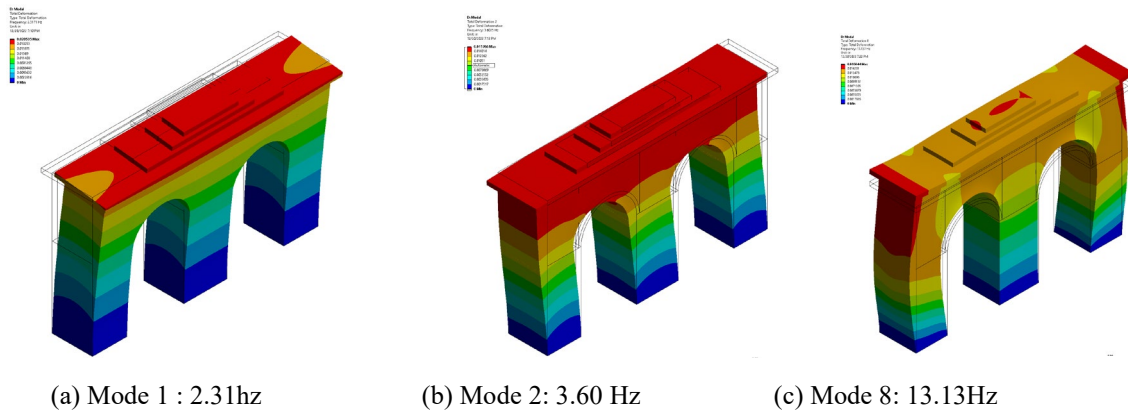


**Fig. 8.** Dominant mode shapes and natural frequencies of the Perry Memorial Arch

3.4 Seismic Response: Time-History Analysis

*Ground motion selection and input direction*

Nonlinear time-history analysis was performed to evaluate seismic response under recorded earthquake ground motions. Three earthquake records were obtained from the Strong-Motion Virtual Data Center, and only horizontal components were considered. The analysis was conducted using a two-step loading sequence: (1) gravity loading without seismic acceleration, followed by (2) application of base acceleration combined with the pre-existing gravity stress state. Base acceleration was applied separately in the X-direction (out-of-plane) and Z-direction (in-plane), as illustrated in Fig. 9.



*Stress and deformation response at critical locations*

Results indicate that global deformations remained small due to the substantial mass and stiffness of the monument; however, localized stress concentrations developed at critical regions, particularly near the base and at interior corners of masonry walls. Stress contours varied across stone masonry, brick masonry, and concrete components, reflecting differences in stiffness, geometry, and load transfer mechanisms.

Maximum principal stress was evaluated at a representative critical location on the stone masonry surface (node 112557, **Fig. 12**). **Fig. 13** compares time-dependent stress response under out-of-plane (X-direction) and in-plane (Z-direction) excitation for PGA values between 0.10g and 0.16g, while **Table 11** summarizes peak stress values. Under out-of-plane excitation, peak stresses were 41.12 psi (0.10g), 131.13 psi (0.12g), 95.64 psi (0.14g), and 206.13 psi (0.16g). Under in-plane excitation, corresponding values were 64.6 psi (0.10g), 110.57 psi (0.12g), 267.58 psi (0.14g), and 217.25 psi (0.16g). The response is clearly direction-dependent, with in-plane excitation producing higher stress demand at intermediate PGA levels, particularly at 0.14g. Given the limited tensile capacity of unreinforced masonry, these stress levels suggest that tensile cracking is plausible at localized regions under higher seismic demand, especially near geometric discontinuities and foundation interfaces. This behavior underscores the importance of considering directional seismic effects when evaluating historic masonry monuments. Directional deformation time histories at the same node are shown in **Fig. 14**. While absolute deformation magnitudes remained small, deformation increased with PGA and exhibited direction-dependent trends consistent with the observed stress response. These findings indicate that seismic vulnerability is governed by localized stress amplification rather than global displacement demand.

**Table 11.** Summary of maximum principal stresses under seismic loading

Peak Ground Acceleration (g)	Maximum Principal Stress Out-of-Plane (psi)	Maximum Principal Stress In-Plane (psi)
0.10	64.6	41.12
0.12	110.57	131.13
0.14	267.58	95.64
0.16	217.25	206.13

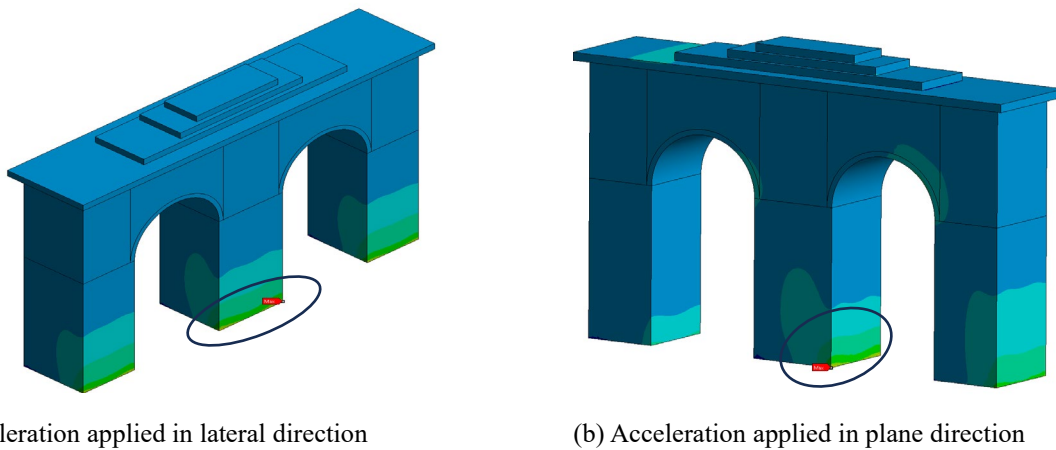
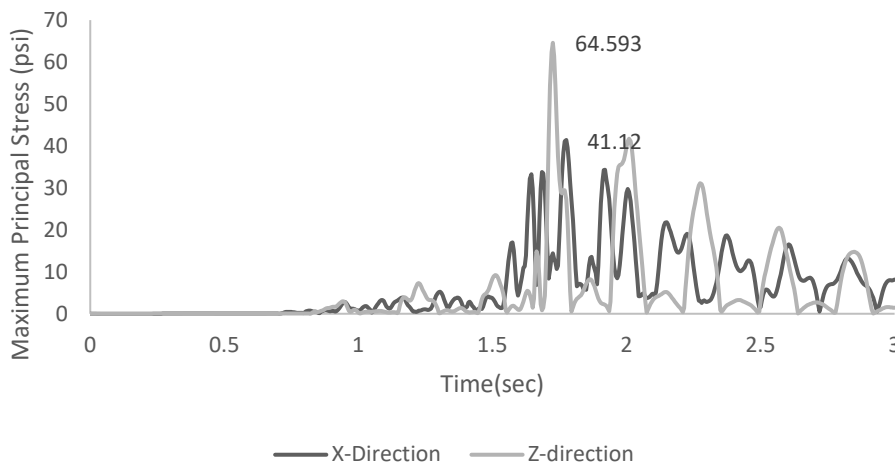
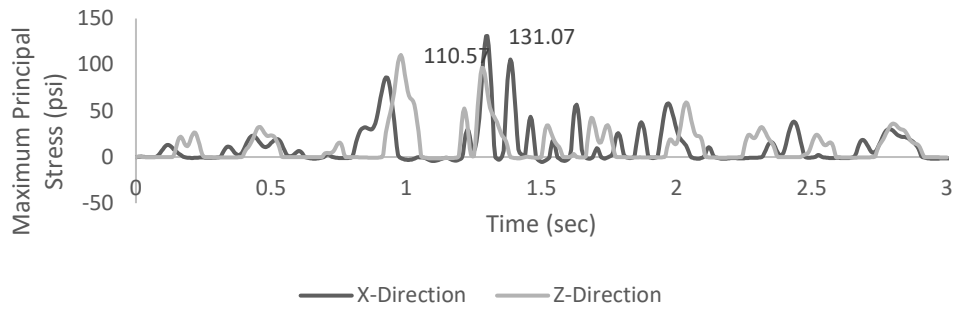


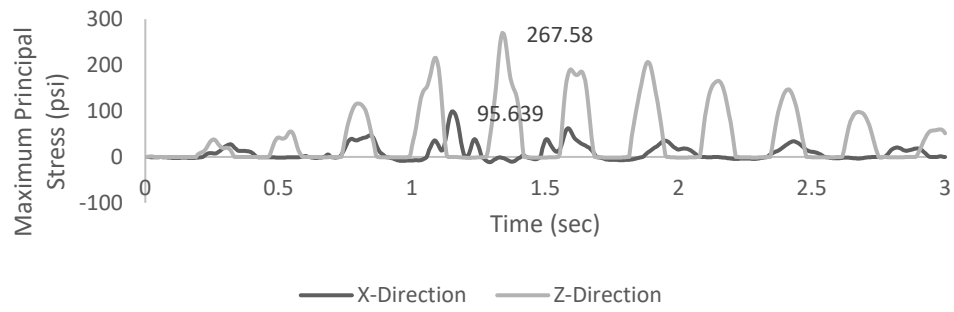
**Fig. 12.** Location of critical node used for stress evaluation



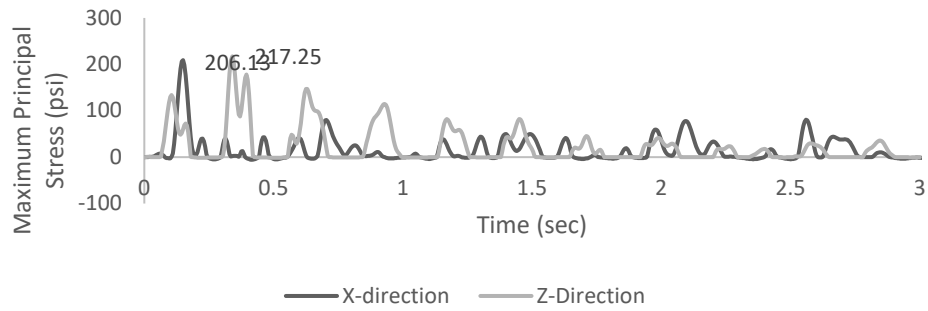
(a) PGA 0.10g



(b) PGA 0.12g

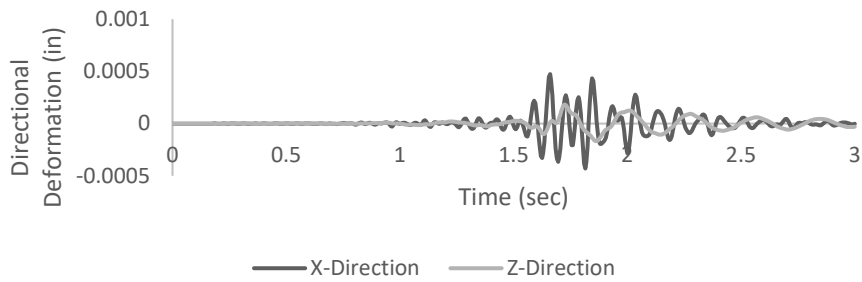


(c) PGA 0.14g

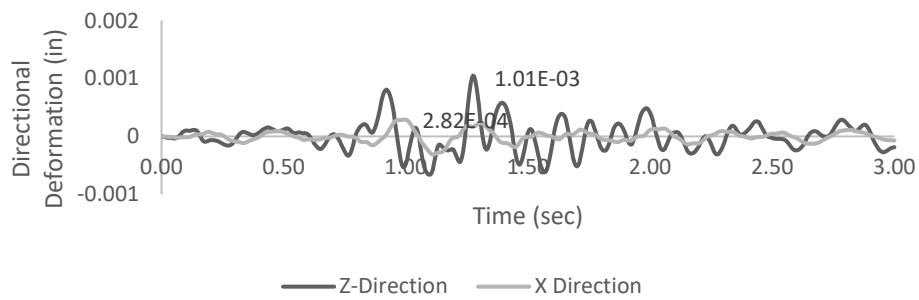


(d) PGA 0.16g

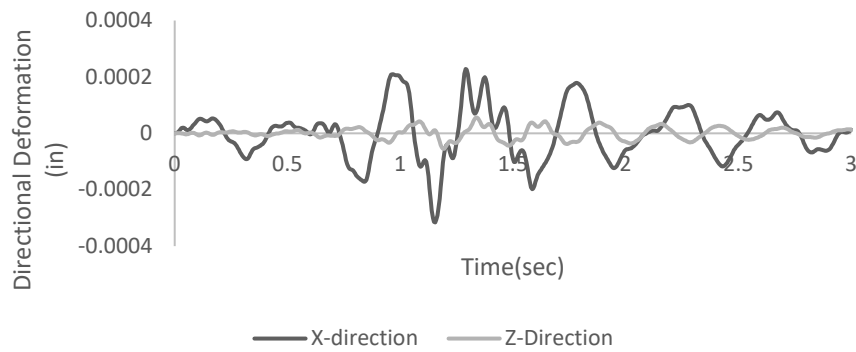
**Fig. 13.** Comparison of maximum principal stress: in-plane vs. out-of-plane excitation



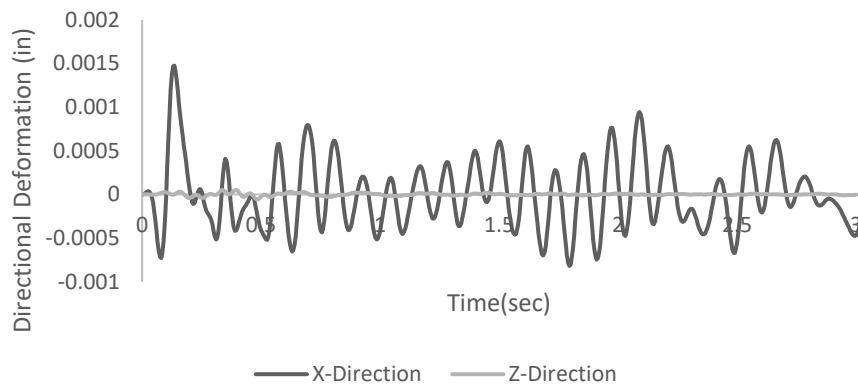
(a) PGA 0.10g



(b) PGA 0.12g



(c) PGA 0.14g



(d) PGA 0.16g

**Fig. 14.** Comparison of directional deformation under in-plane and out-of-plane excitation

#### 4. Conclusions

This study evaluated the structural response of the Perry Memorial Arch under static, wind, and seismic loading conditions using three-dimensional nonlinear finite element modeling. Numerical analyses were performed in ANSYS to investigate stress distribution, deformation patterns, and potential vulnerability zones under gravity loading, lateral wind pressure, modal excitation, and earthquake-induced ground motions derived from historical records. The results provide a screening-level evaluation of the structural performance of this historic masonry monument and offer a technical basis for future preservation and retrofit planning.

The analyses assumed the structure to be in its original condition, with material properties adopted from established literature and design standards. Static gravity load analysis confirmed that stresses remain relatively low throughout most of the structure, indicating that the arch geometry provides substantial compressive capacity and inherent stability under self-weight. This finding is consistent with the load-bearing behavior expected of unreinforced masonry arch systems. Wind load analyses demonstrated that, while the arch can resist extreme wind speeds approaching 239 mph, significant stress concentrations develop at the base and support regions, suggesting that localized material distress or cracking could precede global instability under extreme wind events.

Dynamic analyses revealed that the structural response is strongly influenced by load direction and intensity. Modal analysis showed that the first several vibration modes dominate the response, with significant mass participation in both in-plane and out-of-plane directions. Nonlinear time-history analyses using ground motions with Peak Ground Acceleration (PGA) values ranging from 0.10g to 0.16g indicated that the arch performs satisfactorily under moderate seismic demand. Specifically, the structure remained stable for PGA values up to 0.12g in both the X (out-of-plane) and Z (in-plane) directions. At higher PGA levels, increased stress concentrations were observed at critical joints and support regions, particularly in the Z direction, highlighting directional vulnerability associated with the geometry and load path of the masonry components.

Based on the numerical results, the following conclusions are drawn:

1. The arch geometry provides strong resistance to gravity loads, confirming the effectiveness of its compressive load-bearing mechanism.
2. Extreme wind loading induces elevated stress levels at critical support regions, which may compromise structural integrity under severe wind events.

3. Seismic excitation in the out-of-plane direction represents a governing vulnerability mechanism for the structure, particularly at higher PGA levels.
4. The structure demonstrates adequate seismic resilience for PGA values up to 0.12g in both principal directions.
5. For PGA values of 0.14g and higher, significant stress amplification occurs, especially in the in-plane (Z) direction.
6. Overall structural stability is maintained under low-to-moderate seismic demand typical of the northeastern United States.

Although seismic events are relatively infrequent along the U.S. East Coast, this study illustrates that historic masonry structures can experience meaningful stress demands even under moderate ground motions. These results reinforce the importance of seismic screening assessments for heritage structures located in regions of moderate seismicity. The findings provide valuable insight into the behavior of the Perry Memorial Arch and similar masonry monuments subjected to combined static and dynamic actions.

This investigation represents a preliminary, screening-level numerical assessment. Material properties were assumed, boundary conditions were simplified, and no in-situ testing or ambient vibration measurements were available for model calibration. Accordingly, the numerical results should be interpreted as indicative rather than definitive. Future research should include non-destructive material testing, dynamic field measurements, and model updating to improve predictive accuracy. In addition, targeted retrofit strategies, such as localized masonry strengthening, improved connection detailing, or selective seismic isolation concepts, should be explored to enhance long-term resilience while maintaining the historic integrity of the monument.

## References

- AISC (2017). Steel construction manual (15th ed.). American Institute of Steel Construction.
- American Standard Building Code Requirements for Masonry (1954). Building code for masonry structures. United States.
- ASCE (2016). Minimum design loads and associated criteria for buildings and other structures (ASCE/SEI 7-16). American Society of Civil Engineers.
- Belytschko, T., Liu, W.K., Moran, B., & Elkhodary, K. (2014). Nonlinear finite elements for continua and structures. Wiley.
- Betti, M., Galano, L., & Coisson, E. (2012). Seismic analysis of historic masonry buildings: The Vicarious Palace in Pescia (Italy). *Buildings*, 2(2), 63–82. <https://doi.org/10.3390/buildings2020063>
- Brandão, F.M. (2018). Dynamic characterization of a heritage construction from the 19th century. *Revista Engenharia e Construção*, 11(1), 1–11. <https://doi.org/10.1590/s1983-41952018000100004>
- Chanmalai, T., Chang, B., Misaro, K., Hagos, S., & Hanumanthareddy, T.B. (2021). Development of a nomogram to predict the contact stress between an I-girder and a support roller. *Engineering Solid Mechanics*, 9, 377–390. <https://doi.org/10.5267/j.esm.2021.7.001>
- Chang, B., Bourland, M., Couch, T., Zou, H., & Jung, T. (2015). Evaluation of Texas superheavy-load criteria for bridges. *Journal of Performance of Constructed Facilities*, 29(4). [https://doi.org/10.1061/\(ASCE\)CF.1943-5509.0000667](https://doi.org/10.1061/(ASCE)CF.1943-5509.0000667)
- Chang, B., Phares, B.M., Zou, H., & Couch, T. (2014). Thermal analysis of highway overhead support structures. *Transportation Research Record: Journal of the Transportation Research Board*, 2406(1), 32–41. <https://doi.org/10.3141/2406-04>
- Cook, R.D., Malkus, D.S., & Plesha, M.E. (2001). Concepts and applications of finite element analysis (4th ed.). Wiley.
- De Angelis, A.A. (2020). Seismic vulnerability assessment of a monumental masonry building. *Infrastructures*, 5(11), 93. <https://doi.org/10.3390/infrastructures5110093>
- Lourenço, P.B. (1996). Computational strategies for masonry structures (Ph.D. Thesis). Delft University of Technology, The Netherlands.
- Ong, C., Chang, B., & Lee, J. (2020). Thermal-induced fatigue of overhead truss structures. *Journal of Performance of Constructed Facilities*, 34(2). [https://doi.org/10.1061/\(ASCE\)CF.1943-5509.0001416](https://doi.org/10.1061/(ASCE)CF.1943-5509.0001416)
- Özmen, A.S. (2018). Seismic assessment of a historical masonry arch bridge. *Journal of Structural Engineering & Applied Mechanics*, 1(3), 195–209. <https://doi.org/10.31462/jseam.2018.01095104>
- Petersen, M.D., Mueller, C.S., Moschetti, M.P., Hoover, S.M., Llenos, A.L., Ellsworth, W.L., Michael, A.J., Rubinstein, J.L., McGarr, A.F., & Rukstales, K.S. (2016). 2016 one-year seismic hazard forecast for the Central and Eastern United States from induced and natural earthquakes. U.S. Geological Survey Open-File Report, 2016–1035.
- Puncello, I., & Caprili, S. (2023). Seismic assessment of historical masonry buildings at different scale levels: A review. *Applied Sciences*, 13(3). <https://doi.org/10.3390/app13031941>
- Thongchom, C., Mirzai, N.M., Chang, B., & Ghamari, A. (2022). Improving the CBF brace's behavior using I-shaped dampers: Numerical and experimental study. *Journal of Constructional Steel Research*, 197. <https://doi.org/10.1016/j.jcsr.2022.107482>
- Trifunac, M.D., & Brady, A.G. (1975). A study on the duration of strong earthquake motion. *Bulletin of the Seismological Society of America*, 65(3), 581–626. <https://doi.org/10.1785/BSSA0650030581>
- USGS (2023). OSHPD seismic design maps. <https://www.seismicmaps.org>

Zienkiewicz, O.C., Taylor, R.L., & Zhu, J.Z. (2013). *The finite element method for solid and structural mechanics* (7th ed.). Elsevier.



© 2026 by the authors; licensee Growing Science, Canada. This is an open access article distributed under the terms and conditions of the Creative Commons Attribution (CC-BY) license (<http://creativecommons.org/licenses/by/4.0/>).